Live-cell single-molecule analysis of β_2-adrenergic receptor diffusion dynamics and confinement

Niko Schwenzer[a], Hendrik Bussmann[a], Sebastian Franken[a], and Hanns Häberlein[a, 1]

[a]Institute of Biochemistry and Molecular Biology, University of Bonn, Nussallee 11, 53115 Bonn, Germany

This manuscript was compiled on October 14, 2018

Signal transduction mechanisms and successive regulatory processes alter the lateral mobility of β_2-adrenergic receptor (β_2-AR). In this work we combined modern single particle tracking methods in order to analyze the diffusion dynamics of SNAP-tagged β_2AR in HEK 293 wild-type cells and HEK 293 β-arrestin knockout cells before and after agonist stimulation. For analysis of trajectories we first used mean squared displacement (MSD) analysis. Secondly, we applied an advanced variational Bayesian treatment of hidden Markov models (vbSPT) in combination with the recently introduced packing coefficient (Pc), which together provided a detailed model of three discrete diffusive states, state transitioning and spatial confinement. Interesting to note, state switching between S3 (fast-diffusing) and S1 (slow-diffusing) occurred sequentially over an intermediate state S2. After ligand stimulation more SNAP-tagged β_2AR in HEK 293 wild-type cells switched occupancy into the slow-diffusing state, whereas less receptors were found in the fast diffusive state. Unexpectedly, all three states showed a fraction of confined receptor mobility that increased under stimulation, but confinement sizes were unaffected. Receptor diffusion characteristics were comparable in HEK 293 β-arrestin knockout cells under basal conditions and only minor but non-significant changes occurred upon stimulation, as expected from the depletion of β-arrestin, an important regulatory protein. The data presented here on the occurrence of different diffusion states, their transitioning and variable spatial confinements clearly indicate that lateral mobility of β_2AR is much more complex than previously thought.

SPT | live cell imaging | receptor diffusion | SNAP-tag

G protein-coupled receptors (GPCRs) represent one of the largest protein families in the mammalian genome (1). GPCRs are involved in numerous important signaling processes initiated e.g. by neurotransmitters or hormones. Major mechanisms and regulation of GPCR signal transduction have been discovered (2, 3). One of the most investigated GPCRs is the β_2-adrenergic receptor (β_2AR). Stimulation of β_2AR activates a heterotrimeric G protein, from which the G_s alpha subunit is released to activate adenylate cyclase (AC). AC catalyses the synthesis of the second messenger cyclic adenosine monophosphate (cAMP). Desensitization of β_2AR, achieved by two phosphorylation steps mediated by protein kinase A and G protein-coupled receptor kinase 2, respectively, prevents over-stimulation of the cell. Furthermore, redistribution of phosphorylated β_2AR from functional microdomains into clathrin coated pits followed by receptor internalization reduces receptor density on the cell surface.

However, little is known about the lateral mobility of β_2AR during signal transduction and regulation processes. Immobile, confined, and free diffusion behavior were found possibly characterizing different functional states of adrenergic receptors (4–6). Sungkaworn et al. recently observed immobilization of α_{2A}-adrenergic receptors while interacting with G_s alpha subunits. Interactions of β-adrenergic receptors with scaffold proteins (7) or confinement in caveolae domains (8) are further discussed for varying receptor diffusion properties. Furthermore, desensitized β_2AR receptors interacting with regulatory proteins like β-arrestin, AP-2, and dynamin recruited to clathrin coated pits leads to the formation of an internalization complex (9, 10) with nearly immobile lateral diffusion behavior.

In this work we applied modern single particle tracking methods to analyze the lateral mobility of SNAP-tagged β_2AR in HEK 293 wild-type cells and HEK 293 β-arrestin knockout cells. The latter cell line lacks expression of regulatory adaptor proteins arrestin2 and arrestin3 (9). Fluorescent labeling of β_2AR was realized by expression of SNAP-tag fusion protein (11) in both cell lines combined with the highly specific and photostable dye substrate BG-CF640R (12, 13). Distributions of single β_2AR diffusion coefficients derived from linear fitting of MSD curves of each track were determined. Additionally, all tracks of each condition were evaluated using a software based on a variational Bayesian treatment of Hidden Markov Models (vbSPT) to identify discrete diffusive states and state transitioning probabilities. We also implemented the recently introduced packing coefficient (14) to characterize confined diffusion of receptors.

Significance Statement

G protein-coupled receptors (GPCRs) constitute the largest protein family targeted by approved drugs. In the course of signal transduction, GPCRs undergo various biological states, which correlate to their lateral diffusion behavior and are influenced by functional interactions and the local environment at the plasma membrane. Investigation by single particle tracking has the potential to give insight into open questions about lateral diffusion dynamics. By combination of recent methods, we developed a sophisticated approach that tracks dynamic changes in receptor diffusion and takes their spatial confinement into account. Using these methods, we demonstrate that agonist stimulation of β_2-adrenergic receptor evoked strong alterations to diffusion characteristics, such as increased fractions of slow-diffusing and confined receptors.

N.S. and H.B. performed research; S.F and H.H. designed research; N.S., H.B., S.F. and H.H. wrote the paper

The authors do not declare any conflict of interest.

[1]To whom correspondence should be addressed. E-mail: haeberlein@uni-bonn.de

Materials and Methods

Dye preparation. The fluorescent SNAP-tag substrate BG-CF640R was synthesized by amidization reaction of BG-NH_2 (New England Biolabs #S9148S) and CF640R-NHS ester (Biotium #92108). High-performance liquid chromatography was conducted to purify the desired reaction product (see Supporting Information), as verified by subsequent MALDI-TOF measurement (m/z = 1085.24).

To enrich BG-CF640R, the corresponding HPLC fraction was subjected to a RP-18 solid phase extraction. Phosphoric acid-containing eluent was removed by washing with water. BG-CF640R was then eluted with a mixture of methanol and ethanol. The eluate was dried using a vacuum centrifuge.

A stock solution of BG-CF640R in DMSO was prepared to a concentration of 400 µM and stored at −20 °C. For labeling, the stock solution was diluted in water to a concentration of 4 µM and stored at 4 °C.

Cell culture and transfections. Human embryonic kidney (HEK 293) cells were obtained from DSMZ (Braunschweig, Germany). HEK 293 β-arrestin-KO cells were kindly provided by Asuka Inoue (Graduate School of Pharmaceutical Science, Tohoku University, Sendai 980-8578, Japan). Both cell lines were maintained at 37 °C and 5% CO_2 in DMEM medium (Gibco #31885-023) containing 10% fetal calf serum (Life Technologies #10270), 100 units/ml penicillin and 100 µg/ml streptomycin.

The plasmid coding for SNAP-β_2AR was obtained from New England Biolabs (#N9184). Transfection was done by calcium phosphate transfection method: Cells were seeded in 12-well plates and allowed to attach for at least 24 hours. One µg plasmid DNA was mixed with 6.5 µl of a 2 M aqueous $CaCl_2$ solution and 50 µl sterile water, and then added dropwise to a two fold HBS buffer (pH 7.13, 42 mM HEPES, 274 mM NaCl, 10 mM KCl, 1.4 mM Na_2HPO_4, 15 mM glucose). The mixture was added to the cells after 30 minutes. On the next day, the medium was changed to fresh DMEM containing 750 µg/ml G418 for selection. Individual clones were selected in cloning rings and seeded in distinct wells in a 12-well plate. The clone with the best expression of SNAP-β_2AR was identified by fluorescence microscopy and used for all experiments.

Fluorescence staining and microscopy. For experiments, cells were seeded in 12-well plates on fibronectin-coated glass coverslips using clear DMEM medium (no phenol red, Gibco #11880-028). Coating was performed by preincubating wells prior to seeding, using 500 ng/µl fibronectin in PBS for two hours at 37 °C, then washing twice with PBS. Fibronectin coating improved cell adhesion and growth compared to poly-D-lysine coating, especially in the knockout cell line.

Experiments were performed two or three days after seeding, at a confluency of about 80%. For fluorescence microscopy, SNAP-β_2AR over-expressed in HEK 293 cells were fluorescently labeled by preparing a solution of 2.5 µM BG-CF640R in clear medium and incubating at 37 °C and 5% CO2 for 30 minutes. This was followed by three washing steps with clear medium, and a change to HBSS buffer (Gibco #14025050) for imaging. The coverslip was then placed in a custom made mounting bracket and imaged at room temperature.

Single particle microscopy. Single particle microscopy was performed using an inverted wide-field epi-fluorescence microscope (TE2000- S, Nikon, Kanagawa, Japan), equipped with a 60x water-immersion objective (Plan Apo VC, 1.2 NA, Nikon), a 200-mm-focal-length tube lens, a 4x-magnification lens (VM Lens C-4x, Nikon) and a EMCCD camera (iXon DV-860DCSBV, Andor Technology). For fluorescence excitation, a 637 nm continuous wave laser (Coherent) was set to 20% intensity (0.7 kW/cm^2 in the object plane) using an acousto-optical tunable filter (A.A SA, France). The recording conditions were kept constant for all measurements (1000 frames at 20 Hz, continuous illumination and camera exposure, constant camera gains and readout speeds).

The SNAP-tag labeling procedure described above was altered to achieve sparse labeling. For appropriate spot densities and lower background signal, a five minute incubation using only 10 nM SNAP-tag dye was optimal. After labeling and washing, the cells were immediately imaged at 20 °C and used no longer than 60 minutes. In this time, 20 individual cells were recorded using the following procedure: A cell was centrally positioned in the bright-field channel and focused to the apical membrane. Then, the EM channel and laser were activated and the focus briefly fine-tuned before starting the image acquisition. Cells showing either unusually low spot densities or areal fluorescent artifacts were generally discarded.

Spot tracking. The MATLAB software (version R2016b, MathWorks) was used for the generation of 2D particle tracks from image data and further diffusion analysis. Images were directly imported by the u-track package (15) and processed using the following settings: 1.32 px spot radius, 3 frame rolling window time-averaging for local maxima detection, 2 frame minimum track segment length, 1 frame maximum gap length, other settings on default.

Gaps were afterwards closed by linear interpolation, and the resulting particle tracks pooled by experimental condition and evaluated using scripts described in the following.

Analysis of diffusion behavior. We implemented the package *@msdanalyzer* (16) to calculate mean squared displacement (MSD) values for each track. MSD is calculated as in eq. 1, with r(t) as the particle's position at time t, N as number of positions in the trajectory and $m\Delta t$ as the variable time lag, a multiple of the frame interval.

$$\mathrm{MSD}(m\Delta t) = \frac{1}{N-m}\sum_{i=1}^{N-m}[r(t_i+m\Delta t)-r(t_i)]^2 \qquad [1]$$

Short-term diffusion coefficients of labeled receptors were then derived by linear fitting of the first four MSD points (eq. 2), weighted by number of distances in each MSD value. Tracks of less than 8 frames or low fit goodness ($r^2_{adj} < 0.85$) were excluded.

$$\mathrm{MSD}(m\Delta t) = 4Dm\Delta t \qquad [2]$$

To identify discrete diffusive states from particle tracks, variational Bayes single particle tracking was applied using the vbSPT Matlab package (17). Tracks were thereby segmented and variably classified to one of three states according to their momentary diffusion speed. Although higher order models were recognized by the program, these resulted in higher variance and less distinct states and were therefore not used.

Track simulations and confinement analysis. Tracking data resembling Brownian molecular motion was simulated as follows: 500.000 tracks were generated for each diffusion coefficient (D_1 = 0.011 µm^2/s, D_2 = 0.038 µm^2/s, D_3 = 0.12 µm^2/s) at a frame interval of 50 ms. All generated spots were subjected to localization error by a normally distributed positional offset with σ = 20 nm in each dimension, resembling our experimental setup. To account for photobleaching, the track lengths were modeled by an exponential distribution with μ_{D1} = 21.3 frames, μ_{D2} = 9.8 frames, μ_{D3} = 7.1 frames with a minimal track length of 2 frames. Values for D and µ were derived from averaged vbSPT analysis results of the real data (β_2AR under non stimulating and stimulating conditions).

For the analysis of confinement, the previously classified track segments were extracted and pooled by their respective diffusion states. The recently introduced packing coefficient Pc (14) was used as a measurement of spatial confinement strength. It is defined in a given time window as the sum of squared displacements divided by the squared convex hull area formed by the included particle positions. A window length of 10 positions (0.5 s) was chosen, which should be long enough to yield stable results (see Fig. 5 in (14)) and still include sufficient numbers of track segments. To determine Pc_{95}-values given by the 95th percentile of packing coefficients, random walk data based on the previously determined vbSPT state diffusion coefficients and segment lengths were simulated. The derived Pc_{95}-values were then used as a threshold for spatial confinement. Confined tracks ($Pc > Pc_{95}$) were then compared by their average convex hull areas, again by averaging on the 0.5 s timescale.

Results

Validation of β_2-adrenergic receptor labeling and cell model functionality. Wide-field fluorescent imaging of BG-CF640R

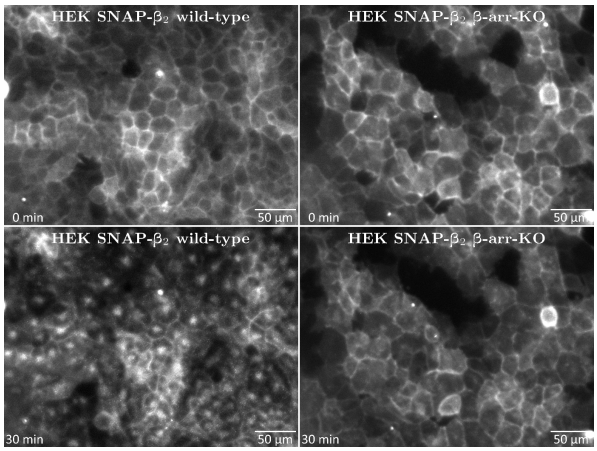

Fig. 1. Fluorescent staining of HEK SNAP-β_2 cells with BG-CF640R in a basal and stimulated state. Isoprenaline (10 µM) was added after the initial image acquisition at t = 0 min. **Top:** In the basal condition, plasma membranes were clearly stained in both genetic backgrounds, indicating expression and membranous location of β_2AR. **Bottom:** Following stimulation in HEK SNAP-β_2 wild-type cells, the membrane staining was displaced by endosomal receptor internalization, as seen in the formation of concentrated fluorescent spots within the cells. This effect was absent in the HEK SNAP-β_2 β-arr-KO cells, which did not show differing receptor distribution following stimulation.

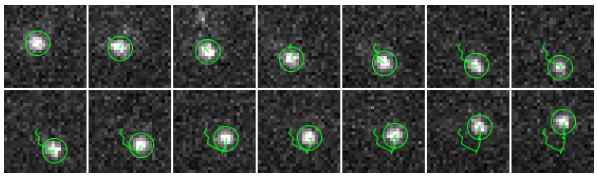

Fig. 2. Example of particle localization and track creation. Shown is a cropped region of 2.6 x 2.6 µm in the apical cell membrane, recorded in 50 ms intervals, in which a freestanding single particle is diffusing. The fluorescent signal of this particle is detected and its origin precisely localized by gaussian fitting. The coordinates are subsequently linked to resemble the path of lateral receptor movement.

labeled HEK SNAP-β_2 cells was performed in wild-type and β-arrestin-KO genetic backgrounds (Fig. 1). Fluorescence intensity corresponding to stained SNAP-β_2 adrenergic receptors was high along the cells plasma membranes. Fluorescent artifacts by non-specific binding were low and cell morphology normal, with no ostensible differences between both genetic backgrounds.

Stimulation of stained HEK SNAP-β_2 wild-type cells with 10 µM isoprenaline, a β-adrenoceptor agonist, led to the formation of concentrated fluorescent spots within cells after 30 minutes, corresponding to early endosomes carrying labeled β_2AR. Following stimulation in HEK SNAP-β_2 β-arr-KO cells, fluorescence was still localized in the plasma membrane after 30 minutes, with no visible formation of early endosomes.

Both dye specificity to SNAP-β_2AR and strongly visible stimulation response of the cells prove the suitability of this model system for single particle tracking. Further, it allows the introduction of newer and more precise evaluation methods, which will be done in the following.

Reduced mobility of β_2-adrenergic receptors after agonist stimulation. For single particle microscopy, the cells were labeled at a much lower dye concentration (10 nM) and incubation time (5 min) to achieve optical separation of single receptor molecules. The movement of single particles in the optically focused apical membrane of individual cells was clearly visible and was recorded for 50 seconds per cell at 20 Hz using an EMCCD camera. Diffusion behavior of labeled receptors under non-stimulating conditions was recorded for 30 minutes. Subsequently, the cells were stimulated with isoprenaline in order to detect alterations in lateral mobility under stimulating conditions, again in a time frame of 30 minutes. Particles were later automatically localized and tracked (Fig. 2). The data of 160 cell measurements were obtained from eight independent experiments and were pooled in respect to genetic background and stimulation condition.

The movement of particles was first analyzed by linear fitting of mean squared displacement curves to receive short-term diffusion coefficients of single particles (Fig. 3). In HEK SNAP-β_2 wild-type cells the labeled β_2AR showed a heterogeneous diffusion coefficient distribution with a median D of 0.060 µm^2/s (N = 2700 tracks). Following stimulation, diffusion coefficients strongly shifted towards low values, reducing the median D to 0.043 µm^2/s (N = 2766). This effect likely corresponds to desensitized receptors prior to internalization (compare Fig. 1).

Evaluation of HEK SNAP-β_2 β-arr-KO cells showed a comparable distribution of β_2AR diffusion coefficients with a lowered median D of 0.053 µm^2/s in the basal state (N = 4909). Under stimulating conditions only a slight shift toward slower diffusion coefficients was observed, with a median D of 0.049 µm^2/s (N = 5147). Thus, the isoprenaline mediated reduction in D of β_2AR depends on the presence of β-arrestins, leading to receptor internalization together with other factors. The difference in observed particle numbers between both genetic backgrounds can most likely be explained by differing expression levels of β_2AR, rather than β-arrestin pathway blockage. Hence, direct comparison of both backgrounds is more ambiguous than analyzing the effects of stimulation, which is prioritized in our experiments.

In a similar experiment that used SNAP-tag labeling of β_2AR in CHO cells, a comparable median D of 0.039 µm^2/s was determined by Calebiro and co-workers (18). Remarkably, isoprenaline stimulation using the same concentration had no effect on diffusivity, which was not further discussed by the authors. We think that endogenous expression of β_2AR in HEK 293 (19) or sufficiently high levels of receptor expression as seen in stable clones may be the deciding factors that lead to receptor desensitization and altered diffusion in our experiment.

A three-state classification model showed consistent values for diffusion coefficients obtained by vbSPT evaluation. The diffusion of β_2AR was further analyzed by applying an algorithm based on variational Bayesian treatment of a hidden Markov model (17), which allowed inclusion of short tracks and detection of intra-track variability. Trajectories were segmented as described by Persson et al. and segments were classified to one of three distinct diffusion states (S1 to S3). Each of these states is defined by diffusion coefficient, occupancy value and state switching probabilities. To maximize model accuracy, data were pooled by condition as before, with 40 cells per analysis. The resulting state diagrams (Fig. 4) showed a similar model in all four conditions. Diffusion coefficients for each state were nearly constant in all conditions and ranged from 0.009 to 0.011 µm²/s (S1), 0.035 to 0.038

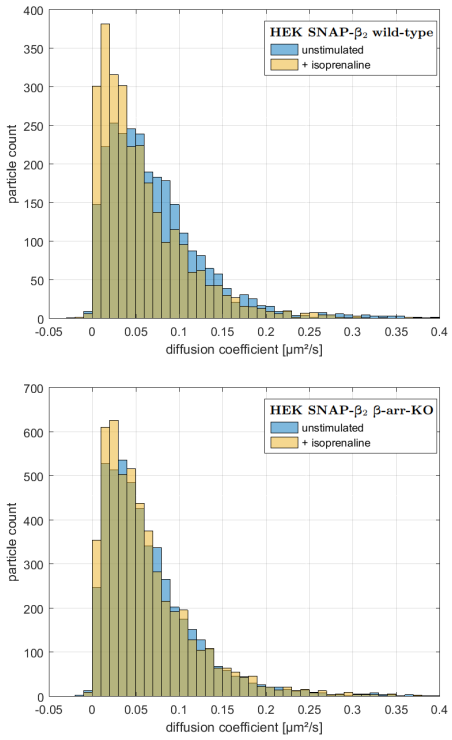

Fig. 3. Distribution of single β_2AR diffusion coefficients in HEK SNAP-β_2 cells, derived by linear fitting of MSD curves. Overlaid in each graph is a blue histogram for the unstimulated condition and a yellow histogram for the isoprenaline-stimulated condition. **Top:** β_2AR in HEK SNAP-β_2 wild-type cells showed a heterogeneous diffusion coefficient distribution with a median D of 0.060 μm²/s. Following stimulation, the proportion of small (D < 0.4 μm²/s) diffusion coefficients strongly increased, reducing the median D to 0.043 μm²/s. **Bottom:** β_2AR in HEK SNAP-β_2 β-arr-KO cells showed a similar distribution pattern with slightly lower basal (unstimulated) values, as indicated by a median D of 0.053 μm²/s. Stimulation resulted in only a slight shift towards lower diffusion coefficients, with a median D of 0.049 μm²/s.

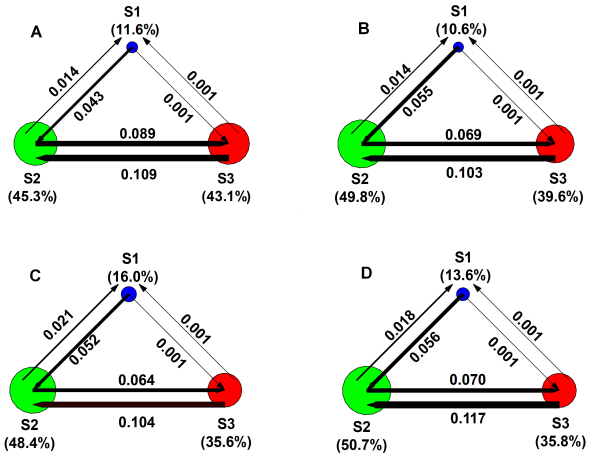

Fig. 4. Diffusion state models for all conditions, attained by vbSPT analysis of pooled track data. **A**: HEK SNAP-β_2 wild-type cells **B**: HEK SNAP-β_2 β-arr-KO cells **C**: A + stimulation **D**: B + stimulation. | Colored circles represent discrete diffusion states S1 to S3 and circle size indicates occupancy. Arrows indicate switching rates between states. Isoprenaline stimulation resulted in major changes in diffusion states, but the underlying diffusion coefficients are not affected. Knockout of β-arrestin clearly reduced the mentioned stimulatory effects.

μm²/s (S2) and 0.116 to 0.123 μm²/s (S3). This consistency demonstrated model robustness and allowed comparison of other metrics associated with the model, namely state occupancy and transition probabilities. For bar graphs and significance testing (Fig. S1-S3), slightly altered data was produced by batch wise data splitting and analysis (4 x 10 cells per condition).

Agonist stimulation altered receptor state occupancies by state switching. In HEK SNAP-β_2 wild-type cells that were stimulated with isoprenaline, occupancy of slow-diffusing state S1 increased from 11.6 to 16.0 %. Similarly, the fraction of receptors in S2 increased from 45.3 to 48.4 %, whereas the fraction of receptors in fast state S3 was strongly reduced from 43.1 to 35.6 %. Only the changes for S1 and S3 occupancy were significant (Fig. S2).

The same trends were seen in HEK SNAP-β_2 β-arr-KO cells, but to a lesser extent: Stimulation increased S1 occupancy from 10.6 % to 13.6 %. Occupancy of S2 was initially higher at 49.8 %, and only increased to 50.7 %. The occupancy of S3 was reduced from 39.6 % to 35.8 %. Although stimulation initiated the same trends that were seen in HEK SNAP-β_2 wild-type cells, the changes here were not significant. Obviously, the subsequent regulation of activated β_2AR in HEK SNAP-β_2 β-arr-KO cells was disturbed, as seen in the missing internalization of β_2AR under stimulating conditions (Fig. 1). We propose that slowed diffusion by altered state occupancies of activated β_2AR (Fig. 3, 4) is caused by the molecular interactions involving β-arrestin, further supported by lack of a significant stimulation response in HEK SNAP-β_2 β-arr-KO cells (Fig. S1-S3).

The observed differences in occupancy between conditions correlate with altered probabilities of state switching of the registered particles (shown by arrows in Fig. 4). Two general observations were made: Regardless of genetic background and stimulation, state switching rates between S1 and S3 were neglectable (P_{13} and $P_{31} <= 0.001$), thus proving sequentiality of state switching. Secondly, P_{23} and P_{32} were consistently much higher than P_{12} and P_{21}, indicating that receptors were more likely to change between the two fast states.

Transition probability ratios between states were calculated as the ratio of forward to backward switching probabilities between adjacent states and revealed significant changes for S2 ↔ S3 transitioning in HEK SNAP-β_2 wild-type cells following stimulation (Fig. S3). A similar finding was observed for SNAP-tagged epidermal growth factor receptor in MCF-7 cells (20). The reduced ratio indicated a stronger preference of receptors for S2 compared to S3. This change was also present, but not significant under β-arrestin-KO. The ratio of S1 ↔ S2 transitioning was lowered in both genetic conditions under stimulation, but the change was not significant.

Diffusion states differed in spatial confinement. To further characterize the nature of each diffusion state, the track segments corresponding to each state were extracted from the full trajectories and subjected to a confinement analysis based on their state and packing coefficient (Pc). The Pc values were calculated for sufficiently long segments using a 10 frame (0.5 s) sliding window, and compared against a 5 % false detection likelihood threshold (Pc_{95}) based on the simulation of random diffusion.

Table 1. Confinement characteristics by diffusion state and stimulation condition in HEK SNAP-β_2 wild-type cells

Unstimulated	S1	S2	S3
Number of segments	522	3015	2614
Confined fraction [%]	68.2	42.7	28.2
Confinement size mean [nm]	59.2	102.2	182.3
	± 11.1	± 13.7	± 23.6
Isoprenaline	S1	S2	S3
Number of segments	993	3779	2478
Confined fraction [%]	74.7	52.2	38.0
Confinement size mean [nm]	56.4	100.6	179.1
	± 10.0	± 14.7	± 24.3

Table 2. Confinement characteristics by diffusion state and stimulation condition in HEK SNAP-β_2 β-arr-KO cells

Unstimulated	S1	S2	S3
Number of segments	970	6023	4445
Confined fraction [%]	73.9	35.7	26.5
Confinement size mean [nm]	54.9	102.6	180.1
	± 10.1	± 15.4	± 25.3
Isoprenaline	S1	S2	S3
Number of segments	1424	7103	4404
Confined fraction [%]	70.2	38.6	29.0
Confinement size mean [nm]	57.4	103.2	181.4
	± 10.4	± 14.9	± 24.8

The results in HEK SNAP-β_2 wild-type cells are shown in Table 1. In basal condition, about two-thirds (68.2 %) of track segments of S1 showed a confined diffusion with a mean confinement size (square root of convex hull area) of 59 nm. Particles in S2 were less often confined (42.7 %) and adhered to a larger confinement size of 102 nm on average. The fast state S3 showed an even smaller fraction of confined trajectory segments (28.2 %) with an increased confinement size of 182 nm. The fact that all states included a degree of confined diffusion and that mean confinement areas were nearly constant for each state regardless of genetic background and stimulatory condition are noteworthy, as previous research often classified states rigidly as either confined or free diffusion.

Unlike the high stability of state diffusion coefficients and also confinement areas, which were hardly changed by isoprenaline stimulation, the confined fraction was increased in each state. Confined diffusion was expected based on the recruitment of β_2AR for the internalization process under stimulating conditions (Fig. 1). This process however does not correspond to the confined fraction of one specific receptor state, since all confined fractions are affected by stimulation. Knockout of β-arrestin (Table 2) lessened the increase of confined fractions following stimulation and even slightly reduced it in S1. Further experiments will hopefully help to establish more detailed biological correspondence for each state. For example, these experiments may use shorter time periods following stimulation, monitor the molecular interaction of receptors, or analyze the diffusion of bound ligands.

Conclusion

The HEK 293 SNAP-β_2 cell system with BG-CF640R labeling was well suited to investigate localization, lateral membrane diffusion and associated confinement patterns of β_2-adrenergic receptors. In addition to a general characterization, stimulation with 10 µM isoprenaline evoked strong changes that could be tracked in a macro- and micromolecular scale by using increasingly sensitive methods: In short, classical fluorescence microscopy showed internalization of membraneous β_2AR following stimulation. In MSD-based analysis of single particle tracks, this was reflected by slowed diffusion in a heterogenous diffusion coefficient distribution. MSD is a classical approach that is heavily averaging and therefore does not reflect all information that is contained in particle trajectories. Since the plasma membrane is a complex and heterogenous environment that continuously influences the diffusion of β_2AR, there is a need for a more sophisticated analysis to resolve the complex lateral mobility. By variational Bayes analysis, we found three underlying diffusion states for β_2AR: A slow state, an intermediate state and a fast state, with constant confinement sizes (57 nm, 102 nm, 180 nm) in each state even under stimulation. Surprisingly, all states including the fast diffusive state had a confined fraction of receptors. These fractions were changed following stimulation, as well as state occupancies, a change that was not seen in previous research. The changes to occupancies result from altered state switching that is exclusively sequential via intermediate state S2. Inter-state transitioning probabilities were strongly in favor of S2, also underlined by the observation of low occupancy in the slow state S1 and high affinity for switching to S2. The data and methods presented contribute to a more precise characterization of physiological states and molecular interactions of β_2AR. We believe that our findings enable the research of fine-grained differences between other conditions that manipulate β_2AR signaling and can easily be adapted to other GPCRs.

ACKNOWLEDGMENTS. We thank Asuka Inoue (Graduate School of Pharmaceutical Science, Tohoku University, Sendai 980-8578, Japan) for kindly providing HEK 293 β-arrestin-KO cells.

1. Hill SJ (2006) G-protein-coupled receptors: Past, present and future. *British Journal of Pharmacology* 147(SUPPL. 1):27–37.
2. Magalhaes AC, Dunn H, Ferguson SS (2012) Regulation of GPCR activity, trafficking and localization by GPCR-interacting proteins. *British Journal of Pharmacology* 165(6):1717–1736.
3. Ranjan R, Dwivedi H, Baidya M, Kumar M, Shukla AK (2017) Novel Structural Insights into GPCR–β-Arrestin Interaction and Signaling. *Trends in Cell Biology* 27(11):851–862.
4. Sungkaworn T, et al. (2017) Single-molecule imaging reveals receptor–G protein interactions at cell surface hot spots. *Nature*.
5. Sieben A, et al. (2009) Alpha-hederin, but not hederacoside C and hederagenin from Hedera helix, affects the binding behavior, dynamics, and regulation of beta 2-adrenergic receptors. *Biochemistry* 48(15):3477–82.
6. Sieben A, Kaminski T, Kubitscheck U, Haeberlein H (2011) Terbutaline causes immobilization of single β2-adrenergic receptor-ligand complexes in the plasma membrane of living A549 cells as revealed by single-molecule microscopy. *Journal of Biomedical Optics* 16(2):026013.
7. Valentine CD, Haggie PM (2011) Confinement of 1- and 2-adrenergic receptors in the plasma membrane of cardiomyocyte-like H9c2 cells is mediated by selective interactions with PDZ domain and A-kinase anchoring proteins but not caveolae. *Molecular Biology of the Cell* 22(16):2970–2982.
8. Rybin VO, Xu X, Lisanti MP, Steinberg SF (2000) Differential targeting of β-adrenergic receptor subtypes and adenylyl cyclase to cardiomyocyte caveolae: A mechanism to functionally regulate the cAMP signaling pathway. *Journal of Biological Chemistry* 275(52):41447–41457.
9. Alvarez-Curto E, et al. (2016) Targeted elimination of G proteins and arrestins defines their specific contributions to both intensity and duration of G protein-coupled receptor signaling. *Journal of Biological Chemistry* 291(53):27147–27159.
10. Cahill TJ, et al. (2017) Distinct conformations of GPCR–β-arrestin complexes mediate desensitization, signaling, and endocytosis. *Proceedings of the National Academy of Sciences* 114(10):2562–2567.
11. Keppler A, et al. (2002) A general method for the covalent labeling of fusion proteins with small molecules in vivo. *Nature Biotechnology* 21(1):86–89.

12. Zanetti-Domingues LC, Tynan CJ, Rolfe DJ, Clarke DT, Martin-Fernandez M (2013) Hydrophobic Fluorescent Probes Introduce Artifacts into Single Molecule Tracking Experiments Due to Non-Specific Binding. *PLoS ONE* 8(9).
13. Bosch PJ, et al. (2014) Evaluation of fluorophores to label SNAP-Tag fused proteins for multicolor single-molecule tracking microscopy in live cells. *Biophysical Journal* 107(4):803–814.
14. Renner M, Wang L, Levi S, Hennekinne L, Triller A (2017) A Simple and Powerful Analysis of Lateral Subdiffusion Using Single Particle Tracking. *Biophysical Journal* 113(11):2452–2463.
15. Jaqaman K, et al. (2008) Robust single-particle tracking in live-cell time-lapse sequences. *Nature Methods* 5(8):695–702.
16. Tarantino N, et al. (2014) Tnf and il-1 exhibit distinct ubiquitin requirements for inducing NEMO-IKK supramolecular structures. *Journal of Cell Biology* 204(2):231–245.
17. Persson F, Lindén M, Unoson C, Elf J (2013) Extracting intracellular diffusive states and transition rates from single-molecule tracking data. *Nature Methods* 10(3):265–269.
18. Calebiro D, et al. (2013) Single-molecule analysis of fluorescently labeled G-protein-coupled receptors reveals complexes with distinct dynamics and organization. *Proceedings of the National Academy of Sciences* 110(2):743–748.
19. Atwood BK, Lopez J, Wager-Miller J, Mackie K, Straiker A (2011) Expression of G protein-coupled receptors and related proteins in HEK293, AtT20, BV2, and N18 cell lines as revealed by microarray analysis. *BMC Genomics* 12.
20. Ibach J, et al. (2015) Single particle tracking reveals that EGFR signaling activity is amplified in clathrin-coated pits. *PLoS ONE* 10(11):1–22.